SOFT ROBOTS

Self-healing soft pneumatic robots

Seppe Terryn,[1,2] Joost Brancart,[2] Dirk Lefeber,[1] Guy Van Assche,[2] Bram Vanderborght[1]*

Copyright © 2017 The Authors, some rights reserved; exclusive licensee American Association for the Advancement of Science. No claim to original U.S. Government Works

Inspired by the compliance found in many organisms, soft robots are made almost entirely out of flexible, soft material, making them suitable for applications in uncertain, dynamic task environments, including safe human-robot interactions. Their intrinsic compliance absorbs shocks and protects them against mechanical impacts. However, the soft materials used for their construction are highly susceptible to damage, such as cuts and perforations caused by sharp objects present in the uncontrolled and unpredictable environments they operate in. In this research, we propose to construct soft robotics entirely out of self-healing elastomers. On the basis of healing capacities found in nature, these polymers are given the ability to heal microscopic and macroscopic damage. Diels-Alder polymers, being thermoreversible covalent networks, were used to develop three applications of self-healing soft pneumatic actuators (a soft gripper, a soft hand, and artificial muscles). Soft pneumatic actuators commonly experience perforations and leaks due to excessive pressures or wear during operation. All three prototypes were designed using finite element modeling and mechanically characterized. The manufacturing method of the actuators exploits the self-healing behavior of the materials, which can be recycled. Realistic macroscopic damage could be healed entirely using a mild heat treatment. At the location of the scar, no weak spots were created, and the full performance of the actuators was nearly completely recovered after healing.

INTRODUCTION

With upcoming, new synthetic materials and the general trend of reducing weight and size in next-generation robots, one subdomain, soft robotics (*1*–*4*), takes robotic compliance to the extreme. These soft robots consist almost entirely of very soft, flexible, deformable materials (*5*), often elastomeric polymers such as Ecoflex (Smooth-On Inc.), which has a modulus of 10^5 to 10^6 Pa. Using these soft materials, an inherent compliance is created, which is comparable to the biological compliance of natural organisms (moduli of 10^4 to 10^9 Pa) (*2*, *3*). This compliance match is key to safely interacting in uncertain and dynamic task environments, including humans. Besides, soft robots can be used to move across rough terrain (*6*, *7*) or enter spaces through tiny cross sections (*8*). When in contact with another object, soft actuators can adapt their shape, making them good candidates for grippers (*9*–*13*) that have to handle soft objects, such as fruits or vegetables.

Because of their intrinsic softness, soft robots are resilient to mechanical impacts (*6*, *14*). However, softness comes at a price: The actuators are susceptible to cuts, shears, and punctures due to sharp objects, and a vast part of soft robotics is pneumatic-actuated, so overpressuring is a common cause of damage. In this research, we propose to solve this weakness by constructing soft robotics from synthetic self-healing (SH) soft materials (*15*) that permit healing microscopic and macroscopic damage. SH materials are a relative recent technology; the term first emerged in 2001 (*16*, *17*). Since then, a wide variety of SH materials has been developed, relying on different physical and chemical principles (*18*–*21*). Some (commercial) applications have appeared in recent years, including SH coatings (*22*) for cars and mobile phone covers that allow healing scratches. SH asphalt and SH concrete are on the verge of a commercial breakthrough (*23*). Puncture SH polymers, already used in SH targets, are promising for aerospace applications (*24*), and artificial stretchable SH films are being developed with high potential for artificial skin applications (*25*, *26*). However, to date, SH material technology has barely made its entrance in robotics, in which SH is only known on the software level (*27*).

Starting from preliminary studies (*15*), we prove that SH polymer networks that are cross-linked through a thermoreversible Diels-Alder (DA) reaction (*28*) can be used to develop soft pneumatic actuators that permit the healing of realistic, macroscopic damage caused by sharp objects or overloading. The DA polymers (*29*) used are in essence nonautonomous SH materials because a trigger is needed to activate the reversibility of the bond formation process. Macroscopic damage can be repaired in a couple of hours using mild heating as a trigger (>70°C). The need for a trigger, such as heat, complicates the healing procedure to some extent. However, it does provide an improved control over the process and a potentially infinite healing capacity. Of course, these nonautonomous SH polymers can be turned into an autonomous SH mechanism by combining them with a system that provides the trigger—in this case, a heating device. Robots are ideal demonstrators for the integration of such an SH mechanism because they contain the power sources and control options required for the trigger system. Other SH polymer approaches, like photoinduced SH polymers (*30*) and supramolecular SH polymers (*31*), certainly have potential for soft robotics too, but these will not be further elaborated here.

In this study, we introduce the SH ability in three applications of soft pneumatic robots. An SH soft hand (Fig. 1, A and D) was developed for applications wherein safe human-robot interactions are demanded, for example, in social robots (*32*), household robots, and hand rehabilitation devices (*33*). Being active in nonpreprogrammed, dynamic environments, they are likely to encounter sharp objects, such as metal edges, shattered glass, sharp plastics, or just the edge of a piece of paper. The fingers of the prototype (Fig. 1, A and D), which are based on existing bending actuator designs (*34*, *35*), are made entirely of flexible SH polymers. Second, an SH soft pneumatic gripper (Fig. 1B) was built using the same material. Because of the flexibility of the bending actuators, the gripper can handle a variety of soft objects without the need for extensive control and has potential for use in sorting and packing lines of, for example, the fruit and vegetable industry (*36*). Sharp objects like broken twigs can find their way into the lines and damage the gripper while sorting.

[1]Robotics and Multibody Mechanics (R&MM), Vrije Universiteit Brussel (VUB), and Flanders Make, Pleinlaan 2, B-1050 Brussels, Belgium. [2]Physical Chemistry and Polymer Science (FYSC), VUB, Pleinlaan 2, B-1050 Brussels, Belgium.
*Corresponding author. Email: bram.vanderborght@vub.ac.be

Downloaded from https://www.science.org at The Hong Kong University of Science and Technology (Guangzhou) on May 26, 2026

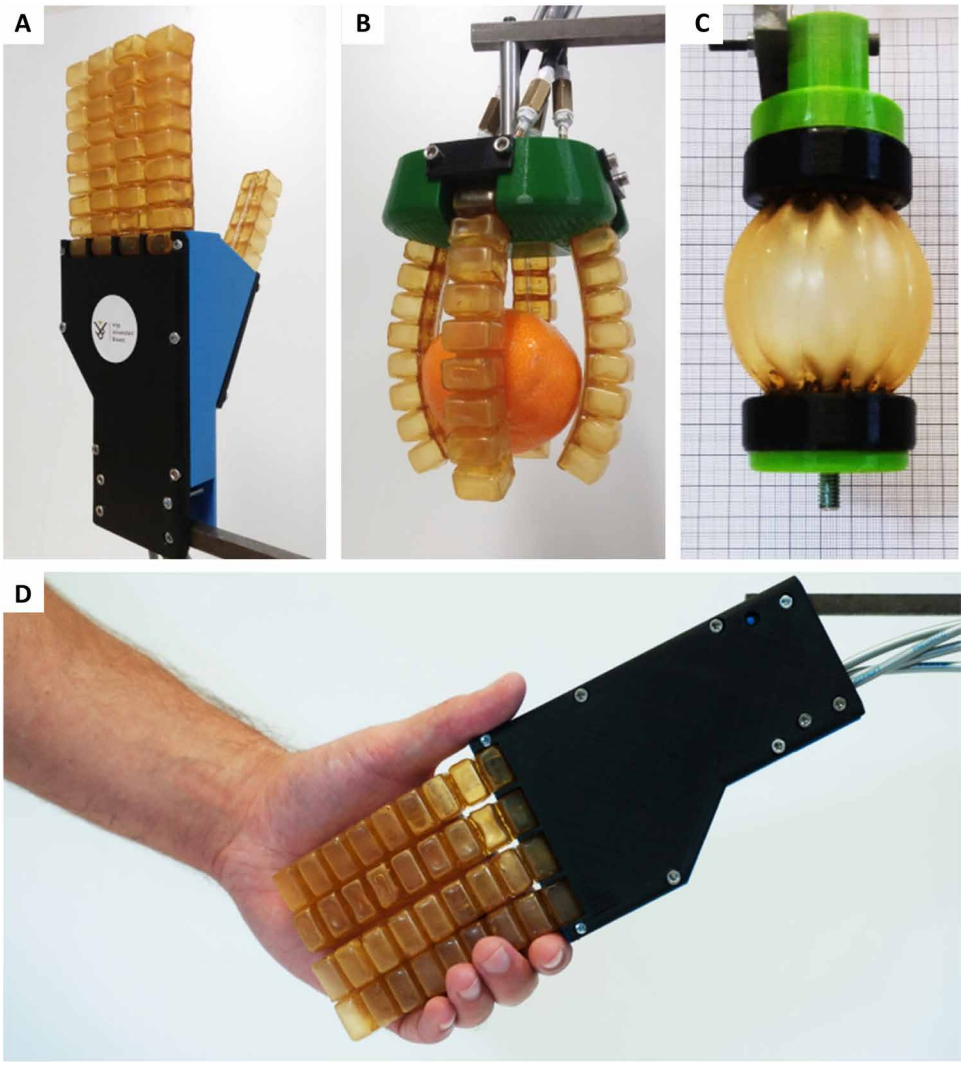

Fig. 1. SH soft pneumatic actuators. (**A** and **D**) SH soft pneumatic hand. (**B**) SH soft pneumatic gripper. (**C**) SH PPAM.

The third application is contractive pneumatic artificial muscles (*37*), often used in antagonistic setups to integrate compliance in robotic systems (*38*). They can produce high levels of forces at low to moderate speeds, excluding the need for (heavy) gearboxes. However, to produce high forces, high overpressures are required, which leads to increased wear and the formation of punctures and leaks, limiting the life cycle of the muscles. To deal with this, two SH pleated pneumatic artificial muscles (PPAMs) (Fig. 1C) (*37*) were built. In all three applications, realistic damages could be healed entirely using an SH procedure requiring mild heat (80°C). No weak spots are created at the location of the scar, and the actuator performances were almost entirely recovered after every healing cycle.

In the search for alternative manufacturing techniques for soft robotics, the reversible network formation that is the basis of the SH ability of DA polymers can be beneficial. Two separated surfaces of DA components can be healed together, as illustrated by the "shaping through folding and self-healing" (*15*) approach used to construct all prototypes. This allows manufacturing DA sheets into single SH parts with a more complex structure: the actuator prototypes. In addition, we illustrate that DA parts with completely different mechanical properties can also be healed together to form single parts. Being manufactured from DA polymers has an additional advantage; the SH parts are remendable and therefore completely recyclable, which will be demonstrated in this paper. Soon, soft robotics will leave the laboratories and enter the industry and our daily environment. We think that it is important that this emerging technology is sustainable right from the start. In general, the use of self-healing/remendable polymers can have a contribution in the development of eco-friendly soft robotics. It can have beneficial impact on the life span of a wide variety of robotic components and reduce their over-dimensioning (*39*), lowering their ecological footprint. In addition, once a robot reaches the end of its usefulness, its SH components can be completely recycled and reused.

The paper presents healing experiments on DA polymer samples to illustrate and describe the SH ability. The viscoelastic and mechanical properties of the synthesized DA polymers are measured, and their potential for soft robotic applications is evaluated. For each SH actuator application, prototypes were designed using finite element modeling and manufactured using a shaping method exploiting the self-healing capacity of the materials. The mechanical performance of the prototypes was measured and compared with that of soft robots in literature, and their healing capacity was evaluated for realistic damage to the membranes of the actuators. The recovery of the properties of the SH polymers and the performance of the soft actuators after multiple SH cycles are validated.

RESULTS

Self-healing based on reversible Diels-Alder bonds

The healing capacity of the soft actuators is based on the DA reactions between a diene (furan) and a dienophile (maleimide) (Fig. 2A) (*29*), which form thermoreversible cross-links in the polymer network (Fig. 2B). The exothermal DA reaction is an equilibrium reaction for which the equilibrium extent of the reaction is a mild function of temperature. The SH procedure can be split into five stages (illustrated in Fig. 3), along with microscopic images of DA polymer samples at the different stages (movie S1). (i) Damage: First, the polymer is damaged, for example, by making a cut with a sharp object or a perforation by applying excessive overpressure. At the location of the damage, the DA bonds are mechanically broken because these are the weakest of the network. (ii) Heating: The healing action is activated by means of a heat stimulus (for our systems, 80°C suffices). By increasing the temperature,

Downloaded from https://www.science.org at The Hong Kong University of Science and Technology (Guangzhou) on May 26, 2026

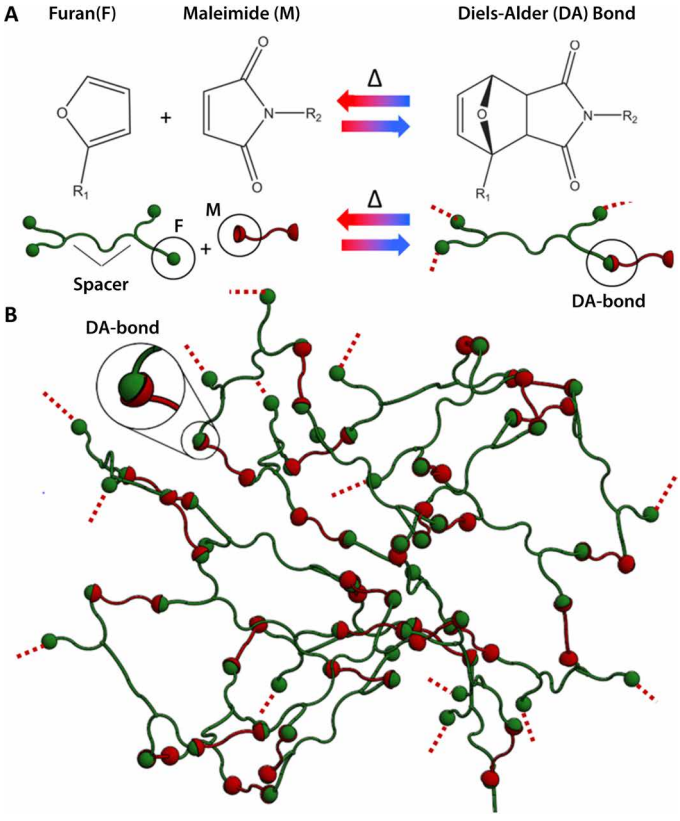

Fig. 2. The thermoreversible network formed by the DA cross-links. (**A**) The equilibrium DA reaction: At low temperatures, the network is formed due to high conversion to the DA bonds. At high temperatures, these DA bonds fall apart, and the mobility of the polymer chains increases. (**B**) Thermoreversible elastomeric network formed by cross-links of the reversible DA bond.

the equilibrium is shifted from a major fraction of formed DA bonds toward the breaking of these bonds and the formation of furan and maleimide functional groups. As a result, the mobility of the polymer chains in the network will be increased. (iii) Isothermal stage: Staying at these temperatures will further increase the mobility by breaking cross-links as the reaction progresses to the new equilibrium, up to a point where the polymer has enough mobility and enough time to seal the gap/cut (typically 20 to 40 min). (iv) Controlled cooling: When the damage is sealed, the temperature can be decreased. Upon cooling, the shift of the equilibrium is reversed, resulting in the gradual reforming of the cross-links in the network (Fig. 2B), which is the basis for restoring the properties of these DA polymers. It is important to perform this with a low-cooling gradient because this enhances the recovery of the initial mechanical properties and reduces the total duration of the SH procedure. (v) Recovery at ambient temperature: At room temperature, the initial mechanical properties have to be fully recovered. Slow cooling followed by a sufficiently long waiting time at ambient temperature offers a good compromise between the decelerating kinetics and the increasing thermodynamic driving force for the formation of the bonds. Using a cooling rate of 2 K min^{-1}, this last step takes around 22 hours according to simulations (fig. S3). The complete temperature profile of the healing can be found in fig. S4.

Table 1. Thermal and mechanical properties of DA materials synthesized using different Jeffamine *Jx* spacers.

Properties		J4000	J2000	J400
Glass (g) and gel transition temperatures				
DMA: Tg	°C	−48.5 ± 0.4	−43.6 ± 2.4	74.7 ± 1.7
Rheology: Tgel	°C	98 ± 1	119 ± 1	
DMA properties: 25°C, 1 Hz, 0.5 % (J4000), 0.5% (J2000), 0.1% (J400)				
Storage modulus	MPa	12.9 ± 1.3	107.4 ± 26.0	1602.5 ± 431.5
Loss modulus	MPa	1.79 ± 0.14	19.3 ± 2.9	79.6 ± 21.7
Tan(δ)		0.139 ± 0.004	0.183 ± 0.021	0.055 ± 0.026
Stress stain curve: 25°C, 65 %/min (J4000 and J2000) 0.1 %/min (J400)				
Fracture strain	%	356 ± 19	353 ± 31	1.58 ± 0.07
Fracture stress	MPa	1.88 ± 0,07	6.85 ± 0.29	20.9 ± 1.8
Young modulus	MPa	5.0 ± 0.1	66.3 ± 5.5	1755 ± 78
Density	g/ml	1.05 ± 0.03	1.13 ± 0.02	1.19 ± 0.01

Thermal and mechanical properties of the Diels-Alder material

The mechanical properties at ambient temperature and during healing can be tuned during the synthesis (fig. S1) of the DA polymer. For this work, the length of the Jeffamine spacer used for synthesizing the furan-functionalized building block (Fig. 2A) was varied (*15*, *29*, *40*). For shorter spacer lengths (400 g mol^{-1}), a polymer network (J400) (Fig. 2B) is created with a higher cross-link density, resulting in a glassy material with a storage modulus of 1.6 GPa and a strain at fracture of only 1.6%. When the spacer length is longer (2000 g mol^{-1} and 4000 g mol^{-1}) , J2000 and J4000-based polymer networks are obtained, respectively. The J4000 results in the most flexible material of the series, with a storage modulus of 13 MPa and a strain at fracture of 360%. A summary of the thermal and mechanical properties of the three basic DA polymers is presented in Table 1 (experimental results can be found in figs. S5 to S8). For the properties wherein an SD is provided, four samples were measured. Many other variations can be made during the synthesis. By combining Jeffamines with different chain lengths, the entire range of mechanical properties between the most flexible J4000 network and the most brittle J400 network can be synthesized. This allows tuning of the DA polymers for diverse robotic applications. In previous work, the brittle J400–based thermoset was used to construct a self-healing mechanical fuse (*39*) that can protect a robotic actuator. The flexible J4000 elastomer is used to construct the soft robots (Fig. 1) in this paper.

Design of the bending soft pneumatic actuator

To demonstrate the potential of DA polymers in existing soft robots, we decided to build a Pneu-Net actuator (*41*). These are made up of a series of channels and chambers constructed in an elastomer, usually a hyperelastic material like Ecoflex 0030 (Young's modulus of 67 kPa). When the chambers are pressurized, they inflate, and motion is created. All kinds of motions are created using different Pneu-Net designs (*7*, *8*, *34*, *41*), but the one mostly used in soft gripper/hand applications (*36*) is the bending soft pneumatic actuator (BSPA) (*35*, *42*). In these applications, the hyperflexible BSPA can easily get damaged by all kinds of sharp objects, making it ideal demonstrators for the introduction of SH DA elastomers in soft pneumatic robotics. A BSPA prototype was designed and constructed almost entirely out of DA polymer (Fig. 4, A and B, and fig. S10).

The BSPA actuator is a cuboid in which a series of nine inflatable air chambers (cells) is embedded. A flexible tube is integrated in the bottom layer that connects all of the nine cells to the same

Downloaded from https://www.science.org at The Hong Kong University of Science and Technology (Guangzhou) on May 26, 2026

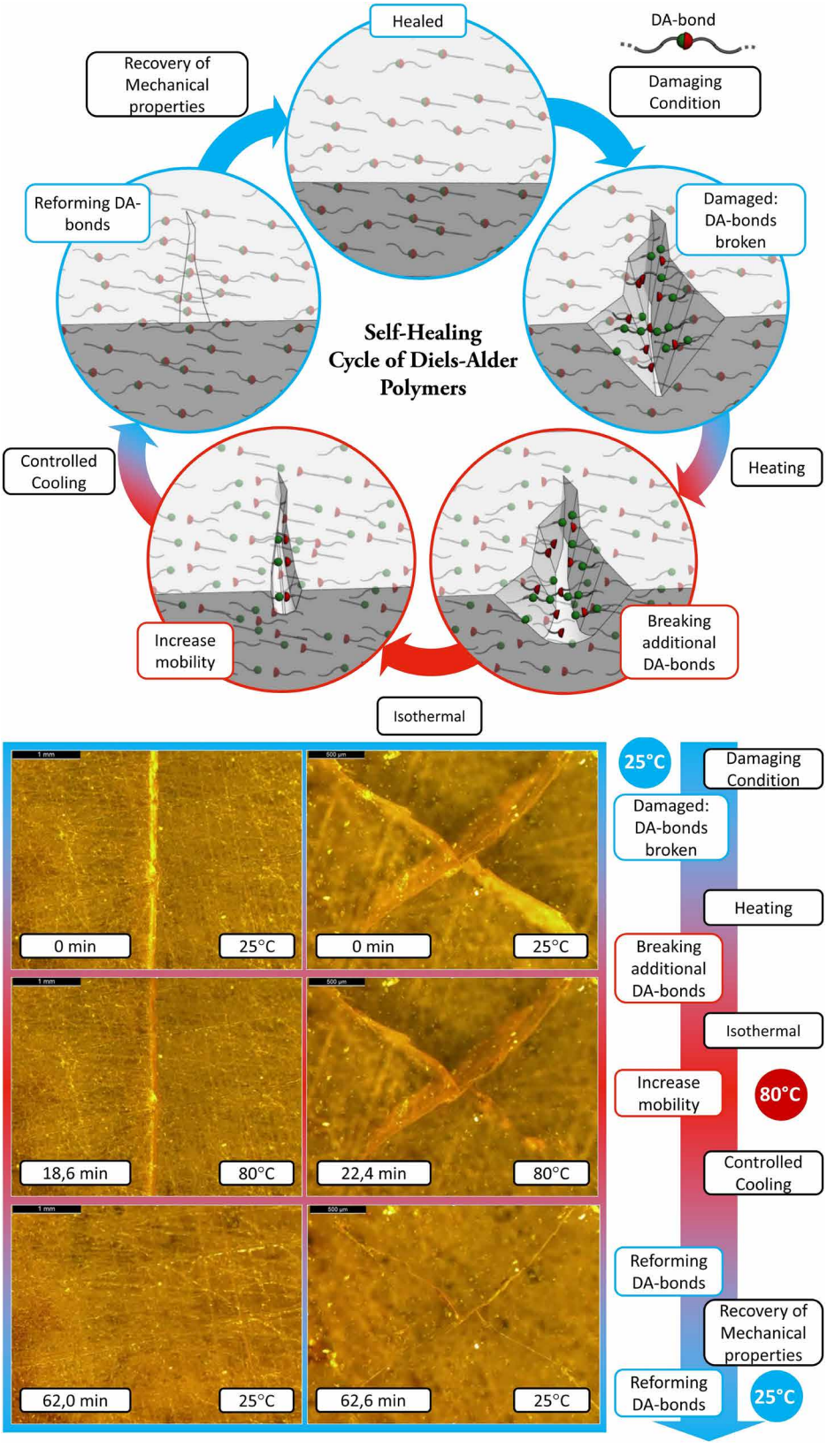

Fig. 3. Schematic of the SH cycle of DA polymers. The SH procedure contains five steps: the damage, a heating step, an isothermal step, a controlled cooling, and a recovery at room temperature. The pictures illustrate the self-healing of a damaged DA polymer sample (DPBM-FGE-J4000) during the different stages (movie S1).

pressure source, such that all can be pressurized simultaneously. The entire actuator is constructed out of the most flexible self-healing DA polymer, the 1,1′-(methylenedi-1,4-phenylene)bismaleimide (DPBM)–furfuryl glycidyl ether (FGE)–J4000, except from the flexible tube that is made out of Tygon R3603. The bottom layer, connecting all chambers and containing the flexible tube, is thicker, allowing very little planar strain. Consequently, pressurization of the air chambers produces inflation on the top and side surfaces, whereas the strain at the bottom surface remains essentially zero. As the expanding outer walls of the cells start making contact, a bending motion is produced (Fig. 4, A and B), where the distance between the two ends of the actuator decreases as the curvature increases. The same principle has led to the development of actuators that respond to pressurization with a wide range of motions: bending, extension, contraction, twisting, and others.

The design was fine-tuned by simulating large deformations, using a static elastic model in Abaqus (Fig. 4C, fig. S9, and movie S2). The elastic deformation response is modeled using the Young's modulus of the DA material (J4000-based, 5.0 MPa) and the flexible tube (1.1 MPa). Because of the relative small strains (less than 30%) and limited pressurization times (typically a few minutes), viscoelastic response effects of the polymers did not have to be accounted for. Gravity was accounted for (densities: J4000, 1.05 g/ml and tube, 1.00 g/ml). Numerical simulations indicated that slightly decreasing the wall thickness of the cells while maintaining a sufficiently rigid bottom sheet results in an increase in curvature of the BSPA. To evaluate this in practice, BSPAs were constructed with a wall thickness of 0.75 (BSPAs 1 and 2) and 0.60 mm (BSPAs 3 and 4) (fig. S10).

Shaping soft robots using the self-healing ability

The SH ability of DA polymers can offer great benefits for the manufacturing of (self-healing) soft robots. We developed a shaping method to produce three-dimensional (3D) polygon structures starting from 2D sheets of SH polymers by combining folding and healing steps. The process, which we named shaping through folding and self-healing (*15*), was used to manufacture all the SH prototypes (Fig. 1) and will be illustrated with the shaping process of the BSPA (Fig. 4E). In total, four healing steps were needed to develop the prototype.

Downloaded from https://www.science.org at The Hong Kong University of Science and Technology (Guangzhou) on May 26, 2026

After synthesis of the building block, the DA material is solvent-cast into sheets (figs. S1 and S12). To construct the cells of the SPA, we cut a plus sign out of a J4000-based sheet. The plus-shaped geometry is folded into an open rectangular cuboid shape. The sides of the cuboid are sealed and made airtight by subjecting the cuboid to a heat treatment in an oven (2 hours at 78°C, cooling at ±0.5 K min^{-1}), using the SH ability. A single cell is formed by closing the box using a slightly larger square of the J4000-based sheet. The cell is made airtight by locally heating the joints up to 110°C for seconds only (using a soldering tool). To complete the actuator, nine cells are placed in series and are fixed to a bottom J4000-based sheet containing the flexible tube using a third SH procedure (30 min at 78°C, cooling at ±0.5 K min^{-1}). An additional local heating was used to make sure that the bottom sides were completely airtight.

Because the thermoreversibility of the different DA polymers originates from the same reversible DA cross-links, polymers with completely different mechanical properties can be fused together to form a single part, using their SH ability, while the connection becomes as strong as the materials themselves. Figure 5 shows optical microscopy images of the edge of a J4000-based and a J2000-based sheet that are fused together in healing procedure (movie S3). The initial gap (0.3 mm) at the top of the two sheets was completely sealed. The surfaces of the two sides were also smoothed because microscopic scratches were also healed. The fact that combining different DA polymers is perfectly feasible strongly increases the degree of freedom during the design phase of soft robotics because single parts can be created, consisting of materials with different properties.

Mechanical properties of the soft pneumatic actuator

Four BSPA prototypes were constructed and characterized using a dedicated test setup containing a pressure control system (figs. S14 and S15). The characteristics of the four BSPAs can be found in Fig. 6 (A to C). The variation in behavior between SPAs 1 and 2 and SPAs 3 and 4 is due to the difference in sheet thickness of the cells, which are 0.75 and 0.60 mm, respectively (fig. S10). The deformations of the actuator were captured for various overpressures using a digital camera (Fig. 4B). The four bending actuators follow nearly the same curvature trajectory (Fig. 6A), which is necessary for soft hand and soft gripper applications in which a well-controlled movement is required.

The bending angle α, defined in Fig. 4B, is presented as a function of the overpressure in the air chambers in Fig. 6B. BSPAs 1 and 2 have very similar characteristics, which is also the case for BSPAs 3 and 4.

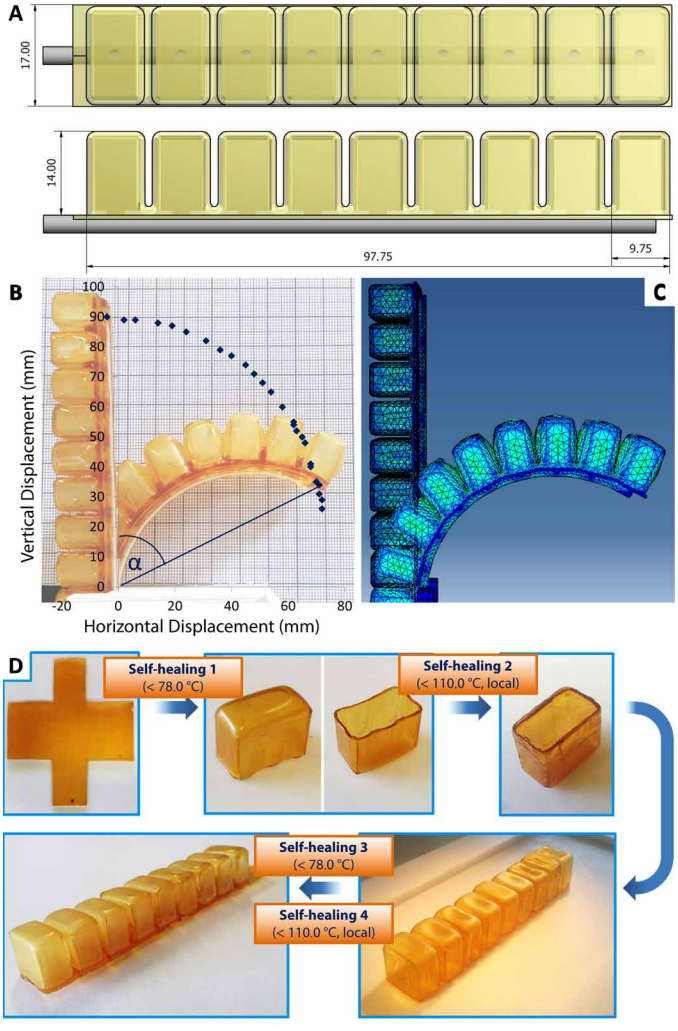

Fig. 4. Design and manufacturing of the SH BSPA. (**A**) Dimensions (in millimeters) (detailed data sheets in fig. S10). (**B**) Illustration of the bending motion caused by an overpressure in the air chambers. (**C**) Abaqus simulation for large deformations at 30 kPa (fig. S9 and movie S2). (**D**) Building the BSPA: Through folding and self-healing procedures (<78°C globally and <110°C locally), connections are made between the different parts, and the actuator is made airtight (fig. S12).

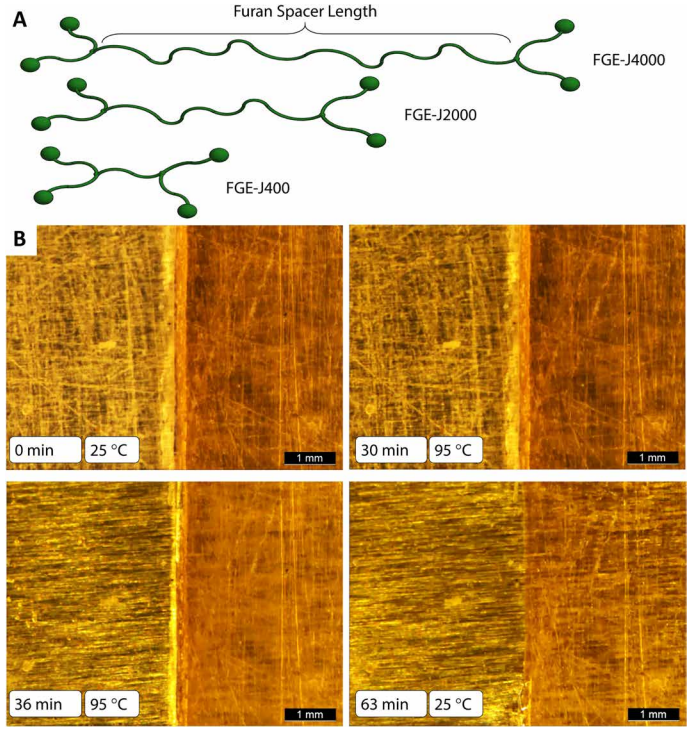

Fig. 5. DA sheets with completely different mechanical properties can be seamlessly healed together. (**A**) Using different Jeffamines (J400, J2000, and J4000), furan-functionalized building blocks (FGE-*Jx*) with different spacer lengths can be synthesized. (**B**) Because the J4000 and J2000 DA polymers differ only in furan spacer length, the materials can be self-healed together using an SH procedure with a maximum temperature of 95°C (movie S3). The initial gap between the sheets was 0.3 mm.

Downloaded from https://www.science.org at The Hong Kong University of Science and Technology (Guangzhou) on May 26, 2026

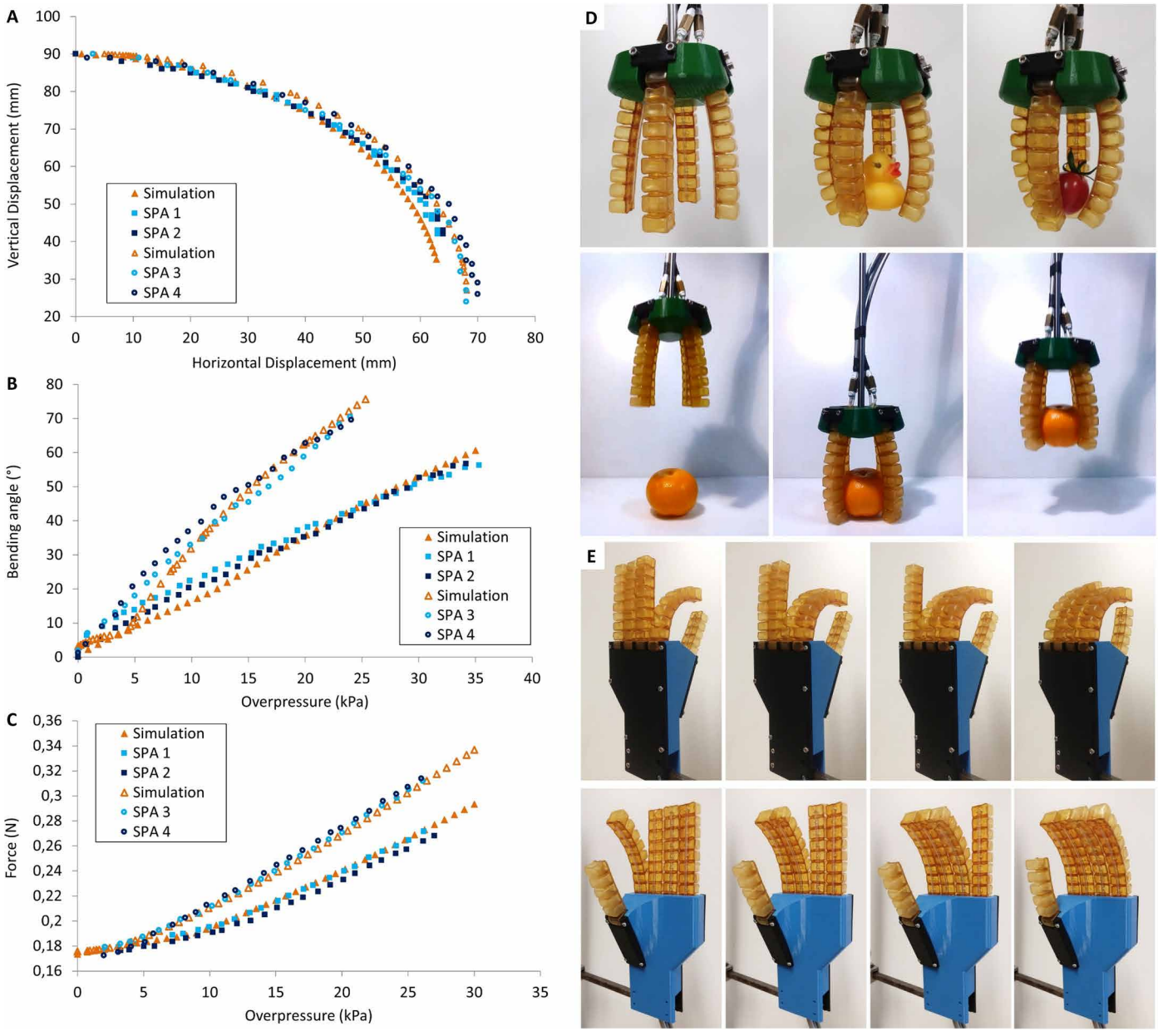

Fig. 6. Mechanical characteristics of the four BSPAs and their functionality in a soft gripper and a soft hand. The experimental measurements are compared to the numerical simulations using static elastic models in Abaqus. (**A**) Vertical and horizontal displacement of the actuator tip for different overpressures. (**B**) Bending angle as a function of the overpressure. (**C**) Force exerted by the tip of the BSPA. (**D**) Operating the four BSPAs in a soft pneumatic gripper. The overpressure in the actuators can be regulated individually. This allows simultaneously exerting the same force on the object with each actuator to create smooth, controlled grasping motions. Soft objects, such as an orange (92.8 g), can be grasped, picked up, and moved (movie S4). (**E**) The four BSPAs were also integrated as fingers in a soft pneumatic hand, together with a six-cell prototype acting as a thumb. All actuators are controlled individually (movie S5).

This indicates that shaping through folding and self-healing allows producing bending actuators in a reliable manner. Bending angles of up to 70° could be achieved for overpressures around 25.0 kPa, and decreasing the wall thickness leads to more flexible, softer actuators. The force exerted by the tip of the bending actuators on a surface was measured for different overpressures (Fig. 6C). Forces of about 0.25 and 0.32 N were registered for 25.0 kPa. The low modulus (5.0 MPa) of the materials is the main factor for the softness of the grip. To validate the static elastic finite element models (FEMs) in Abaqus (fig. S9) and the polymer characterization, we simulated the deformations and forces of the BSPAs as function of different overpressures and compared these to the experimental results (Fig. 6, A to C). For both BSPA designs, the experimental results agree very well with the simulation outcomes.

SH soft pneumatic actuators in application

To validate the functionality of the SH-BSPAs, we used four in a gripper application (Fig. 1B) and five in a soft hand (Fig. 1, A and D). To control the actuator movement in these two applications, we built a setup in which

Downloaded from https://www.science.org at The Hong Kong University of Science and Technology (Guangzhou) on May 26, 2026

five overpressures can be regulated individually using five control systems (figs. S14 and S15). The soft pneumatic gripper was developed by placing the four bending actuators in a 3D printed part (Fig. 6D). The constructed gripper was subjected to tests gripping different soft items, including mandarin oranges, a rubber duck, and cherry tomatoes (Fig. 6D). Using the control setup, the overpressure in the actuators can be regulated individually such that the force exerted by the four actuators on the soft object is almost identical at all times. A smooth, controlled grasping motion that allows picking up of the different soft objects is created, as illustrated for the mandarin orange that weights 92.8 g (movie S4). These tests indicate that the SH-BSPAs and, more specifically, the DA elastomers used have an adequate flexibility and mechanical stability for use in soft gripper applications.

In an alternative application, four nine-cell BSPAs were placed together with a six-cell prototype, created to act as a thumb, on a 3D printed part to form a soft pneumatic hand (Fig. 6E and movie S5). Because the actuators can be controlled individually, the soft hand can be used by a social robot to make gestures and to grasp soft objects. The soft actuators will ensure safe human-robot interactions in a dynamic task environment. The SH capacity of the BSPA is validated further in the paper.

Design of the pneumatic artificial muscles

Different types of pneumatic artificial muscles have been developed, of which the McKibben muscle (*43*) is the most well known. It contains an elastomeric inner membrane that will expand when inflated, through an elastic strain of the membrane, while a braided sleeving transfers tension. The expansion and contraction of the membrane displays hysteresis, which leads to a decrease in efficiency. In search of higher efficiencies, we developed PPAMs (*37*, *44*), having a working principle that is different from others like the McKibben muscle (*43*). The membrane of the PPAM has a folded structure. In between the folds, cables that transfer tension are arranged. When pressurized, the muscle will expand and contract as a result of the unfolding of the pleats. Because the elastic deformation in PPAMs is limited, their efficiency is increased.

Because pneumatic muscles are usually constructed out of flexible membranes, wear, punctures, or overpressures can damage the muscle and create leaks. In this study, we developed self-healing muscles by constructing the PPAM membrane using the flexible DA polymers, such that damage can be healed using a mild heat treatment. Two prototypes (Fig. 7A and movie S6), PPAM 1 and PPAM 2, were elaborated in DPBM-FGE-J4000 and differ in the depth of the folds. The membrane has a thickness of 0.75 mm; the lengths of PPAM 1 and PPAM 2, not including the fittings, are 55 and 65 mm, respectively; and the muscles have a width of 36 and 33 mm (specific dimensions in fig. S11). To transfer the tension, we placed nylon cables in between the folds. The manufacturing process that is used is again based on the shaping through folding and self-healing technique (fig. S13).

For the two designs, the deformation resulting from overpressuring the muscle is simulated through a static elastic model in Abaqus (Fig. 7A, fig. S9, and movie S2). As for the BSPA, the simulation is limited to the elastic deformation response, modeled using the Young's modulus of the J4000-based DA polymer (5.0 MPa) and the nylon cables (100 MPa). Gravity was accounted for (densities: J4000, 1.05 g/ml and nylon cables, 1.15 g/ml). The unfolding of the membrane as a result of applying an overpressure was captured using a digital camera (Fig. 7A and movie S6).

Mechanical properties of the pneumatic artificial muscles

The pressure in the muscles was regulated with the control system developed for the soft gripper and the soft hand (figs. S14 and S15).

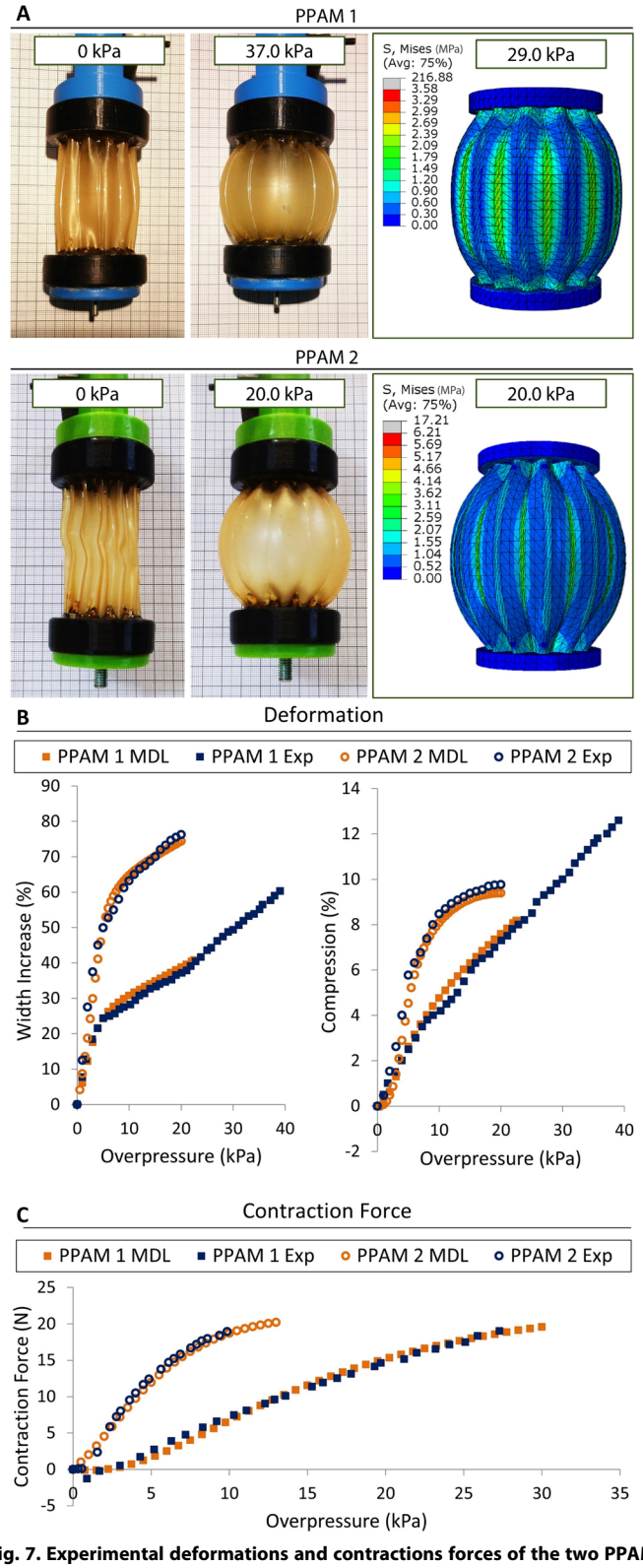

Fig. 7. Experimental deformations and contractions forces of the two PPAM designs. (**A**) Shape of the PPAM at ambient pressure and near-maximum overpressure tested (movie S6). The experiments (Exp) are compared with the results of the numerical simulations using the static elastic model (MDL) in Abaqus (movie S2). (**B**) Relative width increase and contraction as a function of the overpressure. (**C**) Contraction force as a function of the overpressure.

Downloaded from https://www.science.org at The Hong Kong University of Science and Technology (Guangzhou) on May 26, 2026

The increase in relative width of the membrane and the relative contraction of the muscle were measured as a function of the overpressure. The deformation response consists of two phases. Even at low pressures, the membrane starts to unfold, and the width of the muscle and the contraction increase rapidly. At higher pressures, the membrane is entirely unfolded, and the width increases slowly through the elastic straining of the membrane, increasing the contraction. Because the depth of the folds of PPAM 2 is bigger, the first phase results in larger deformations for similar overpressures. The small, negative force at very low pressures in PPAM 1 is due to the nylon cables that are not fully tightened, a problem that will be solved after the first healing cycle.

The contraction force was measured using a load cell (Futek LSB200, 15 lb) and is presented as a function of the overpressure in Fig. 7C. Forces of up to 20 N were registered for pressures as low as 10.0 kPa. An additional advantage of the PPAM, compared with other pneumatic muscles like the McKibben, is that the response does not display a threshold pressure required for functioning (*37*, *44*, *45*). This makes them attractive for low pressure applications. As for the BSPAs, the deformations and the (contraction) forces of the PPAM designs were simulated using the static elastic Abaqus model (Fig. 7B). Again, the experimental results coincide with the outcomes of the simulations for both designs. The operational properties of the two prototype PPAMs indicate that the DA flexible self-healing polymers can be used to develop working pneumatic muscles with adequate performances for low pressure applications.

Self-healing of the actuators

The soft gripper, the soft hand, and the two muscle prototypes demonstrate that the flexible DA polymers have mechanical properties (Table 1) suitable for soft robotics. To evaluate the SH ability, we made cuts in the soft parts of the actuators using a scalpel blade with a thickness of 0.39 mm (Fig. 8, A and B). In future applications of the actuators in nonpreprogrammed, dynamic environments, they are more likely to be damaged when pressurized. This is the case not only for punctures and perforations due to high overpressures or wear but also for damage caused by sharp items. When inflated, a pointy object can more easily slice through the membrane. For this reason, all the cuts were made when the actuators were inflated. When the actuator is inflated and a cut or perforation takes place, it will deflate and the pressure will drop. Thus, by checking the pressure needed to control a certain position, the health of the actuator can be monitored. If the damage is limited, the BSPAs and the PPAMs will, to some degree, keep working after being punctured, making them robust in use. However, the deformation and the (contraction) force generated by the actuators depend on the pressure. Because of leaks, the maximum pressure will decrease, reducing the deformation, force, and contraction performances. More air mass will be consumed to compensate the leakage, increasing the energy consumption and hence decreasing the efficiency of the robot. Moreover, the pressure buildup will be slower, and the dynamic performances will be reduced. Therefore, ability to self-heal is an important characteristic to restore the performances.

Because heating is required for the nonautonomous healing process, it can be performed at a desired time. A damaged actuator can, for example, still be active at a lower efficiency for a limited time, after which it can be healed when the setup is put offline (e.g., at night). To initiate the healing process, the overpressure can be decreased to zero by the control system, and the actuator can be completely deflated. In its noninflated state, the soft pneumatic actuator has a self-sealing capacity: The formed cut or fracture surfaces will be naturally pressed together again, providing contact for the healing procedure. As long as the fracture surfaces are brought back in contact, healing is possible; however, if material is missing, this might no longer be feasible.

To confirm the SH ability of the fingers of the soft pneumatic hand, we made cuts ranging from 8 to 9.5 mm long in the inflated cell walls using a scalpel blade (Fig. 8A and movie S7). After applying damage, the actuator was deflated, and the macroscopic cut was sealed autonomously. Subsequently, the actuator was subjected to a heating procedure in an oven (maximum temperature of 80°C; detailed temperature profile in fig. S4). After this SH procedure, the damage was completely healed, and the actuator was again airtight. The only thing that is left of the incident is a small scar on the surface of the cell wall due to microscopic misalignment of the fracture surfaces. A similar procedure was followed with the two PPAM prototypes. Again, cuts of 8 to 9.5 mm were made with a scalpel blade in the soft membrane (Fig. 8B and movie S8). These could be healed by placing the muscles in the oven, which followed the same temperature profile (fig. S4). As for the BSPAs, all cuts could be healed entirely, and only small superficial scars remained.

Besides sealing the damage, it is important that the mechanical properties of the actuators are recovered after the healing procedure. BSPA 3 was repeatedly damaged by cutting the tip cell with the scalpel blade (as in Fig. 8A; length of cuts ranging from 8 to 9.5 mm) and healed using the procedure mentioned above (fig. S4). After each damage-healing procedure, the actuator was characterized again by measuring the bending deformation as a function of the overpressure in the cells. This damage-heal-measure cycle was repeated twice. Figure 8C plots the bending angle as a function of the overpressure before healing, after one SH cycle, and after two SH cycles. We noticed that repeatedly healing damages using the heating procedure does not influence the actuators trajectory: The results are very similar, and, taking into account minimal variations in the position of the actuator in the test setup, it can be concluded that the mechanical properties of the bending actuator were recovered after each SH cycle.

After the first damage-heal-measure cycle, the BSPA 3 was pushed to its limits by gradually increasing the overpressure. The actuator failed at 24.2 kPa but not at the location of the scar. A perforation took place on the side of one of the cells (indicated with an asterisk in Fig. 8A). Also, this perforation was sealed and made airtight using the SH procedure. Upon pressurizing until failure after the second damage-heal-measure cycle, the BSPA failed at 25.0 kPa, at a third location, on the side of another cell. From these tests, we concluded that no weak spots are created on the location of scars and healed perforations.

To validate the recovery of the properties of the self-healing artificial muscles, PPAM 1 was repeatedly damaged by making a cut all the way through the membrane with the scalpel blade (Fig. 8B) and healed for three times in total. After each healing process, the isometric contraction force was measured as a function of the overpressure in the muscle (Fig. 8D) and compared to the characterization curve of the undamaged PPAM. After the first damage-heal cycle, the characterization curve shifted somewhat downward. This is due to a slight deformation of the membrane because the muscle was manufactured horizontally but healed vertically in the oven. Because this was done vertically, the nylon cables are tightened, which can be seen in the absence of the negative threshold pressure, as seen in the initial curve. Between the first, second, and third cycles, there is only a slight variation in the curves. The curve moves slightly upward with every damage-heal cycle due to a minor change in material properties explained in the next section.

Downloaded from https://www.science.org at The Hong Kong University of Science and Technology (Guangzhou) on May 26, 2026

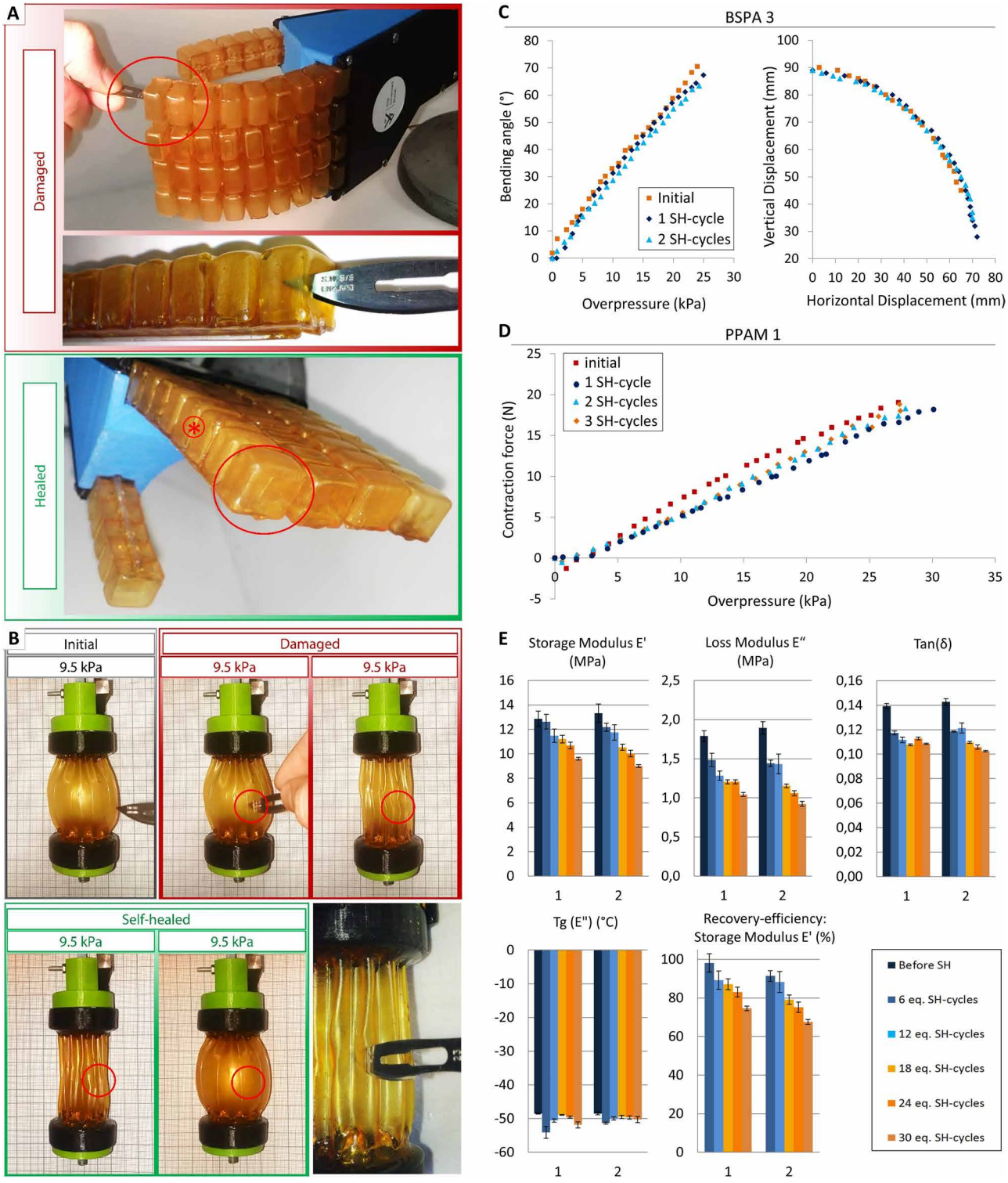

Fig. 8. Validating the SH ability in practice and recovery of the mechanical properties of the actuators after healing cuts. Cuts with lengths of 8 to 9.5 mm made with a scalpel blade. (**A**) Cutting the finger actuator (BSPA) with a scalpel blade with a thickness of 0.39 mm (movie S7). The macroscopic cuts (length of 9.4 mm and all the way through) can be healed entirely using an SH procedure, after which the actuator is again completely airtight. The asterisk indicates the location of failure due to overpressure. (**B**) Macroscopic cuts (8.6 mm) in the self-healing membrane of the PPAM can be healed entirely using an SH procedure (movie S8). After this, the muscle is again airtight and recovers its functionality. (**C**) The bending angle as a function of overpressure and the trajectory of the tip of the BSPA are measured after 1 and 2 damage SH cycles and are compared with the initial characteristics. (**D**) Contraction force of the PPAM 1 as a function of overpressure as measured after 1, 2, and 3 damage SH cycles and compared with the initial characteristics. (**E**) Influence of the heating procedure (4 hours at 80°C followed by at least 3 days at 25°C) on the viscoelastic properties expressed in equivalent SH cycles.

Downloaded from https://www.science.org at The Hong Kong University of Science and Technology (Guangzhou) on May 26, 2026

Self-healing efficiency

The influence of the heating procedure on the mechanical properties of the DA polymer and their repeated recovery was examined. To do so, six series of each four samples for two different batches of the J4000-based DA polymer were prepared. All samples, except the reference series, were subjected to a heating procedure (4 hours at 80°C followed by at least 3 days at 25°C), which can be considered the equivalent of six SH procedures based on the isothermal step (Fig. 3) that has a duration of 40 min (fig. S4). For one series, this heating procedure was performed once, for the next twice, for the third three times, etc., giving an equivalent of 0, 6, 12, 18, 24, and 30 SH cycles. For each series, dynamic mechanical analysis (DMA) was used to measure storage modulus, loss modulus, tan(δ), and the glass transition temperature (Fig. 8E).

For every 4 hours spent at 80°C, the equivalent of six SH cycles, the storage modulus, the loss modulus, and tan(δ) lower a bit, whereas the glass transition temperature remains more or less the same (Fig. 8E). The reproducibility of the observed decreasing trends was shown by the similarity between the results of batches 1 and 2. The small drop might point to a limited decrease in cross-link density resulting from the formation of irreversible bonds through two side reactions in the network: the Michael addition of amine impurities to maleimide groups and the homopolymerization of bismaleimide, both occurring at higher temperatures (fig. S16). These side reactions imply that some of the furan functionalities can no longer form a DA bond, resulting in a gradual decrease of the cross-link density and modulus after healing. The recovery efficiency, defined as $(E'_{\text{initial}} - E'_{\text{xSH cyles}})/(E'_{\text{initial}})$ is, on average, 93.4% for one 4-hour heating cycle (Fig. 8E). Projecting this on a 1-hour SH cycle, a high recovery efficiency of 98 to 99% is reached. The small increase in flexibility results in the small increase in the contraction force of the PPAM actuator observed for the second and third SH cycles (Fig. 8E). We believe that the Michael addition has the largest influence because this reaction occurs at lower temperatures compared to homopolymerization. The recovery efficiency can be increased by working with a bismaleimide with higher purity and by avoiding the presence of unreacted amine, reducing the Michael addition.

Recycling of the self-healing material

To illustrate the recyclability of the DA polymers, we cut cells that could be used in a BSPA (as in Fig. 4D) into pieces and subsequently dissolved them in $CHCl_3$ (fig. S17). Swelling and further dilution decrease the concentration of the DA adduct, gradually shifting the equilibrium to the unbound state. To accelerate the dissolution step, we raised the temperature to 65°C. The obtained solution could be solvent-cast into a sheet again. Similar to the SH procedure, the recycling procedure involved a heating step during solvent-casting. Therefore, a slight drop in storage modulus (E' = 10.5 MPa) compared to the initial properties (E' = 12.9 MPa) is displayed, resulting in a recovery efficiency of 81% (more details in fig. S18). This change in properties can be reduced if bismaleimide is used with higher purity. The recycled sheet (fig. S17) was used to manufacture parts of the six-cell BSPA, the thumb of the soft hand. This proves that the SH soft robotic parts can be recycled.

DISCUSSION

The use of flexible material in robotics opens up new opportunities: Soft robotics can perform tasks in uncertain, dynamic environments without the need for extensive control systems. Their intrinsic softness makes them ideal for safe interactions with their surroundings, which can include people. However, softness and flexibility also imply an increased vulnerability to all kinds of sharp objects and edges found in the uncertain environments in which these robots will function, which is also valid for soft organisms, as a matter of fact. However, if an organism's injuries are limited and given time, they can recover from their injuries. This work has successfully introduced a similar healing ability in soft robotics, more specifically in soft pneumatic actuators. Flexible SH DA polymers, consisting of a thermoreversible covalent network, were synthesized and used to manufacture prototypes for three different self-healing soft robotic applications: a soft gripper, a soft hand, and artificial muscles.

The healing action of these DA polymers can be activated by means of a mild heat stimulus. Macroscopic damage in DA sheets, such as millimeter-long cuts all the way through made with a scalpel blade, can be successfully healed by heating the parts to 80°C for 40 min and slowly cooling down to 25°C (-2 K min^{-1}). After 24 hours at 25°C, the initial properties are almost entirely recovered. In the synthesis phase, the mechanical properties can be tuned to fit a wide variety of properties desired for different robotic applications. In this work, a series of three polymers that differs in spacer length and resulting mechanical properties was synthesized. However, many other variations are feasible. Because their SH ability is based on the same reversible DA cross-links in their network structures, sheets or parts with completely different mechanical properties can be seamlessly healed together, which can be beneficial in the soft robotics manufacturing process. The mechanical characterization of the flexible DA polymers displays properties adequate for soft robotics applications.

The most flexible polymer of the DA series, DPBM-FGE-J4000, was used in our current SH soft robotic applications. For all three soft pneumatic systems—the soft gripper, the soft hand, and the artificial muscles—the design was supported by simulating large deformations using a static elastic FEM in Abaqus. To build the prototypes, we developed a manufacturing process involving folding and self-healing, which exploits the SH ability of the DA polymers. Flexible DA sheets are first folded into 3D polygon structures. The creases can be made permanent and the joints airtight by subjecting the part to a mild heating procedure (<80°C globally and <110°C locally). Using this technique, soft actuators, such as the fingers of the soft hand, can be made as a single part and almost entirely out of SH material.

The performance of the SH prototypes was experimentally validated using dedicated test benches that contain pressure regulating systems, a digital camera, and force and pressure sensors. The measured performance, deformations, and forces resulting from pressurizing the membrane are adequate for soft robotic applications and coincide with the results from the FEM simulations. The SH capacity of the prototypes was verified by healing realistic macroscopic damage applied to the membrane. Using a scalpel blade, relatively large cuts were made all the way through the membranes of the pressurized actuators. Because of the self-sealing ability of the pneumatic actuator under noninflated condition, the cut surfaces are naturally pressed together. When subjected to an SH procedure (maximum temperature of 80°C), all cuts were healed, leaving nothing but a small scar behind (due to microscopic misalignment). At the location of the scar, the membrane was again airtight, and no weak spots were created.

It is crucial that after the healing operation, the performance of the actuator is recovered. For this reason, the actuators were repeatedly damaged, healed, and tested, showing that the performance is almost entirely restored. There is only a very small change for the PPAM actuators due to a slight increase in the flexibility of the DA elastomers after each healing cycle. The storage modulus of the flexible DA polymer

Downloaded from https://www.science.org at The Hong Kong University of Science and Technology (Guangzhou) on May 26, 2026

is recovered with 98 to 99%. Because slow side reactions are thought to be at the origin, in this case the maleimide homopolymerization, this recovery efficiency might be increased by using bismaleimide with higher purity in the synthesis and avoiding tertiary amines that catalyze the homopolymerization.

An additional advantage of the DA polymers is that they are recyclable, either by remolding them or by dissolving them in a suitable solvent. 3D polygon waste structures of the DA polymer were cut into small pieces and subsequently dissolved. Through solvent-casting, recycled sheets could be created, with a recovery efficiency of the storage modulus of 81%, an efficiency that might again be increased by reducing the occurrence of side reactions using bismaleimides with higher purity. Recycled sheets were used to manufacture the thumb of the soft hand. Therefore, DA polymers have potential to support an ecological transfer from a laboratory setting to an industrial-scale and to our daily environment.

This study illustrates through demonstrators that self-healing DA elastomers can be used for a variety of soft robotic applications. Because of SH capacity given to the actuators, different types of damage to the membranes can be healed using mild heating procedures. This SH principle increases the life span of soft robotic components while their over-dimensioning, previously used to withstand damaging conditions, can be reduced.

MATERIALS AND METHODS

Reagents

FGE (96%) and DPBM (95%) were obtained from Sigma-Aldrich (fig. S1). The Jeffamine D series [poly(propylene glycol) bis(2-aminopropyl ether)] with average degree of polymerization n [as determined by nuclear magnetic resonance (NMR)] were obtained from Huntsman and have the following characteristics: J400: $n = 6.9$, $M_n = 477$ g mol^{-1}; J2000: $n = 44.2$, $M_n = 2640$ g mol^{-1}; J4000: $n = 71.1$, $M_n = 4200$ g mol^{-1}. Chloroform (stab./Amylene) (minimum of 99.9%) was obtained from Biosolve Chimie. All chemicals were used as delivered.

Synthesis of the DA polymers

FGE is reacted with a stoichiometric amount of Jeffamine Jx (x = 400, 2000, or 4000), yielding a furan-functionalized compound with functionality 4 (FGE-Jx). This reaction was performed for a minimum of 7 days at 60°C under continuous stirring, after which the reaction was completed for 2 days at 90°C. The functionality of the FGE-Jx compound was 4.0 ± 0.2, as checked by NMR. To produce the DA polymers (details in fig. S1), the furan-functionalized compound (FGE-Jx) was mixed with DPBM in a stoichiometric ratio ($r = n_{Maleimide}/n_{Furan} = 1$) and dissolved in chloroform (20 weight % solution). To ensure complete dissolution of the DPBM in chloroform, the mixture was stirred for 24 hours at 25°C. To form sheets of the thermoreversible networks, the solution is casted in Teflon molds, and the chloroform is evaporated. The chloroform is evaporated by increasing the temperature up to 90°C under vacuum. The thermoreversible network is formed by slowly cooling down the sheet after the chloroform has been evaporated completely.

Measuring of the mechanical behavior

The viscoelastic behavior of the DA polymer networks, DPBM-FGE-J400, DPBM-FGE-J2000, and DPBM-FGE-J4000, were measured on a TA Instruments Q800 DMA for three to four samples per material. Rectangular samples 0.2 to 0.7 mm thick, 1.5 to 3.2 mm wide, and 3.6 to 4.6 mm long were measured in tension mode at a frequency of 1 Hz, an oscillation strain of 0.1%, and a force tracking of 125%, using a heating rate of 10 K min^{-1} (fig. S5). The glass transition temperature is taken as the temperature in which the loss modulus reaches its maximum.

The fracture strain and stress of the different polymers of the DA series were measured at 25°C using stress-strain tests until fracture (fig. S6). The measurements were performed on a TA Instruments Q800 DMA in controlled strain mode with rectangular samples in tension for four samples per materials. For the glassy J400-based material, a rate of 0.1% min^{-1} was used, whereas for the elastomeric J2000- and J4000-based materials, a rate of 65% min^{-1} was used. The samples had a thickness of 0.2 to 0.7 mm, a width of 1.7 to 5.5 mm, and a length of 4.0 to 4.2 mm, adjusted to the mechanical behavior of the materials. The Young's modulus was obtained from a stress-strain curve with a strain ramp of 65% min^{-1} for the J2000- and J4000-based materials and 0.1% min^{-1} for the J400, using a linear regression over the strain interval (J4000: 0 to 5%; J2000: 0 to 2.5%; J400: 0 to 0.2%) (fig. S7).

Temperature profile of the SH process

The SH procedure used in practice to heal the damage to the actuators consists of four phases (fig. S4): The sample is placed in an oven at 80°C where it is heated at about 10 K min^{-1} to 80°C, and it is kept isothermal for about 35 min. Subsequently, the sample is cooled at about 2 K min^{-1} to 25°C, where it is kept for about 24 hours to fully restore the mechanical properties. The temperature profile was optimized using kinetic simulations (fig. S3).

Pressure controlling system

In the setup, five pressures can be regulated by five control systems in parallel (figs. S14 and S15). Each system contains a buffer volume and two solenoid valves (Matrix 720 Series compact), one connected to a pressure source and the other to atmospheric pressure. These are switched at high frequency using pulse-width modulation (PWM)–controlled Power FET Switches (MOSFET 4 v04). The PWM signal is provided by an Arduino Mega ADK board. The pressure signal is measured using a Honeywell Differential Pressure Sensor (15 psi, 10-V dc) and amplified using an instrumentation amplifier of Analog Devices, AD623ANZ. For the force measurements, two different load cells were used (FUTEK LSB200 2 lb and 50 lb). Their signals were amplified using the FUTEK Amplifier Module CSG110.

SUPPLEMENTARY MATERIALS

robotics.sciencemag.org/cgi/content/full/2/9/eaan4268/DC1

Fig. S1. Synthesis of the thermoreversible covalent networks.
Fig. S2. The thermoreversible DA reaction.
Fig. S3. Simulation for the DA series: DPBM-FGE-J400, DPBM-FGE-J2000, and DPBM-FGE-J4000.
Fig. S4. Temperature profile of the SH procedure.
Fig. S5. Temperature-dependent viscoelastic behavior for the DA polymer series measured by DMA.
Fig. S6. Stress-strain curves for the DA polymer series.
Fig. S7. Young's modulus determination of the DPBM-FGE-Jx.
Fig. S8. Measuring the gel temperature (T_{gel}) through dynamic rheometry.
Fig. S9. Simulating different designs for the SH soft robotic demonstrators using a static elastic model in Abaqus.
Fig. S10. Dimensions of the two BSPA designs in millimeters.
Fig. S11. Dimensions of the two PPAM prototypes in millimeters.
Fig. S12. Constructing a BSPA using shaping through folding and self-healing.
Fig. S13. Shaping through folding and self-healing to manufacture the PPAMs.
Fig. S14. Pressure control system scheme.
Fig. S15. Images of the pressure control system.
Fig. S16. Irreversible cross-linking of bismaleimide networks.

Downloaded from https://www.science.org at The Hong Kong University of Science and Technology (Guangzhou) on May 26, 2026

Fig. S17. DA polymer waste of the manufacturing process of the prototypes can be recycled.
Fig. S18. Recovery of the material properties after the recycling procedure.
Movie S1. Visualization of the SH process of the DA elastomers using optical microscopy.
Movie S2. Healing DA polymers together with different mechanical properties; DPBM-FGE-J4000 and DPBM-FGE-J2000.
Movie S3. Simulating large deformations using static elastic models in Abaqus.
Movie S4. The soft pneumatic gripper handling a 92-g mandarin orange.
Movie S5. The soft pneumatic hand in which all the fingers are controlled individually.
Movie S6. Actuation of the PPAM.
Movie S7. Damaging the soft pneumatic hand.
Movie S8. Damaging the PPAMs.

REFERENCES AND NOTES

1. C. Laschi, B. Mazzolai, M. Cianchetti, Soft robotics : Technologies and systems pushing the boundaries of robot abilities. *Sci. Robot.* **1**, 3690 (2016).
2. S. Kim, C. Laschi, B. Trimmer, Soft robotics: A bioinspired evolution in robotics. *Trends Biotechnol.* **31**, 287–294 (2013).
3. D. Rus, M. T. Tolley, Design, fabrication and control of soft robots. *Nature* **521**, 467–475 (2015).
4. D. Trivedi, C. D. Rahn, W. M. Kier, I. D. Walker, Soft robotics: Biological inspiration, state of the art, and future research. *Appl. Bionics. Biomech.* **5**, 99–117 (2008).
5. R. H. Ewoldt, Extremely Soft: Design with rheologically complex fluids. *Soft Robot.* **1**, 12–20 (2014).
6. M. T. Tolley, R. F. Shepherd, B. Mosadegh, K. C. Galloway, M. Wehner, M. Karpelson, R. J. Wood, G. M. Whitesides, A resilient, untethered soft robot. *Soft Robot.* **1**, 213–223 (2014).
7. S. A. Morin, R. F. Shepherd, S. W. Kwok, A. A. Stokes, A. Nemiroski, G. M. Whitesides, Camouflage and display for soft machines. *Science* **337**, 828–832 (2012).
8. R. F. Shepherd, F. Ilievski, W. Choi, S. A. Morin, A. A. Stokes, A. D. Mazzeo, X. Chen, M. Wang, G. M. Whitesides, Multigait soft robot. *Proc. Natl. Acad. Sci. U.S.A.* **108**, 20400–20403 (2011).
9. R. Deimel, O. Brock, A novel type of compliant and underactuated robotic hand for dexterous grasping. *Int. J. Robot. Res.* **35**, 161–185 (2015).
10. E. Brown, N. Rodenberg, J. Amend, A. Mozeika, E. Steltz, M. R. Zakin, H. Lipson, H. M. Jaeger, Universal robotic gripper based on the jamming of granular material. *Proc. Natl. Acad. Sci. U.S.A.* **107**, 18809–18814 (2010).
11. S. Wakimoto, K. Ogura, K. Suzumori, Y. Nishioka, Miniature soft hand with curling rubber pneumatic actuators, in *Proceedings of International Conference on Robotics and Automation 2009 (ICRA'09)* (IEEE, 2009), pp. 556–561.
12. J. Hughes, U. Culha, F. Giardina, F. Guenther, A Rosendo, F. Iida, Soft manipulators and grippers: A review. *Front. Robot. Al.* **3**, 10.3389/frobt.2016.00069 (2016).
13. J. Amend, H. Lipson, The JamHand: Dexterous manipulation with minimal actuation. *Soft Robot.* **4**, 70–80 (2017).
14. R. V. Martinez, A. C. Glavan, C. Keplinger, A. I. Oyetibo, G. M. Whitesides, Soft actuators and robots that are resistant to mechanical damage. *Adv. Funct. Mater.* **24**, 3003–3010 (2014).
15. S. Terryn, G. Mathijssen, J. Brancart, D. Lefeber, G. V. Assche, B. Vanderborght, Development of a self-healing soft pneumatic actuator: A first concept. *Bioinspir. Biomim.* **10**, 046007 (2015).
16. S. R. White, N. R. Sottos, P. H. Geubelle, J. S. Moore, M. R. Kessler, S. R. Sriram, E. N. Brown, S. Viswanathan, Autonomic healing of polymer composites. *Nature* **409**, 794–797 (2001).
17. X. Chen, M. A. Dam, K. Ono, A. Mal, H. Shen, S. R. Nutt, K. Sheran, F. Wudl, A thermally re-mendable cross-linked polymeric material. *Science* **295**, 1698–1702 (2002).
18. D. Y. Wu, S. Meure, D. Solomon, Self-healing polymeric materials: A review of recent developments. *Prog. Polym. Sci.* **33**, 479–522 (2008).
19. B. J. Blaiszik, S. L. B. Kramer, S. C. Olugebefola, J. S. Moore, N. R. Sottos, S. R. White, Self-healing polymers and composites. *Annu. Rev. Mater. Res.* **40**, 179–211 (2010).
20. S. D. Bergman, F. Wudl, Mendable polymers. *J. Mater. Chem.* **18**, 41–62 (2008).
21. M. D. Hager, P. Greil, C. Leyens, S. van der Zwaag, U. S. Schubert, Self-healing materials. *Adv. Mater.* **22**, 5424–5430 (2010).
22. A. Lutz, O. van den Berg, J. Van Damme, K. Verheyen, E. Bauters, I. De Graeve, F. E. Du Prez, H. Terryn, A shape-recovery polymer coating for the corrosion protection of metallic surfaces. *ACS Appl. Mater. Interfaces* **7**, 175–183 (2014).
23. H. Jonkers, Self healing concrete: A biological approach. *Self Healing Mater.* **100**, 195–204 (2008).
24. K. L. Gordon, R. K. Penner, P. B. Bogert, W. T. Yost, E. J. Siochi, Puncture self-healing polymers for aerospace applications. *Conf. NASA Am. Chem. Soc. Natl. Meet. Expo.* **242**, NF1676L–NF12452 (2011).
25. B. C. Tee, C. Wang, R. Allen, Z. Bao, An electrically and mechanically self-healing composite with pressure-and flexion-sensitive properties for electronic skin applications. *Nat. Nanotechnol.* **7**, 825–832 (2012).
26. C. Hou, T. Huang, H. Wang, H. Yu, Q. Zhang, Y. Li, A strong and stretchable self-healing film with self-activated pressure sensitivity for potential artificial skin applications. *Sci. Rep.* **3**, 3138 (2013).
27. M. Yim, W. Shen, B. Salemi, D. Rus, M. Moll, H. Lipson, E. Klavins, G. S. Chirikjian, Modular self-reconfigurable robot systems [Grand Challenges of Robotics]. *IEEE Robot. Autom. Mag.* **14**, 43–52 (2007).
28. Y.-L. Liu, T.-W. Chuo, Self-healing polymers based on thermally reversible Diels–Alder chemistry. *Polym. Chem.* **4**, 2194 (2013).
29. B. Scheltjens, G. Diaz, M. M., B. Joost, V. Assche, G. Van Mele, Thermal evaluation of a self-healing polymer network coating based on reversible covalent bonding. *React. Funct. Polym.* **73**, 413 (2013).
30. B. Ghosh, M. W. Urban, Self-repairing oxetane-substituted. *Science* **323**, 1458–1460 (2009).
31. P. Cordier, F. Tournilhac, C. Soulié-Ziakovic, L. Leibler, Self-healing and thermoreversible rubber from supramolecular assembly. *Nature* **451**, 977–980 (2008).
32. J. Saldien, K. Goris, B. Vanderborght, J. Vanderfaeillie, D. Lefeber, Expressing emotions with the social robot probo. *Int. J. Soc. Robot.* **2**, 377–389 (2010).
33. P. Polygerinos S. Lyne, Z. Wang, L. Fernando, N. B. Mosadegh, G. M. Whitesides, C. J. Walsh, Towards a Soft Pneumatic Glove for Hand Rehabilitation. in *Proceedings of IEEE/RSJ International Conference Intelligent Robots and Systems (IROS)* (IEEE, 2013), pp. 1512–1517.
34. A. D. Marchese, R. K. Katzschmann, D. Rus, A recipe for soft fluidic elastomer robots. *Soft Robot.* **2**, 7–25 (2015).
35. B. Mosadegh, P. Polygerinos, C. Keplinger, S. Wennstedt, R. F. Shepherd, U. Gupta, J. Shim, C. J. W. Bertoldi, G. M. Whitesides, Pneumatic networks for soft robotics that actuate rapidly. *Adv. Funct. Mater.* **24**, 2163–2170 (2014).
36. http://softroboticsinc.com/.
37. D. Villegas, M. Van Damme, B. Vanderborght, P. Beyl, D. Lefeber, Third-generation pleated pneumatic artificial muscles for robotic applications: Development and comparison with McKibben muscle. *Adv. Robot.* **26**, 1205–1227 (2012).
38. B. Vanderborght, R. Van Ham, B. Verrelst, M. Van Damme, D. Lefeber, Overview of the Lucy project: Dynamic stabilization of a biped powered by pneumatic artificial muscles. *Adv. Robot.* **22**, 1027–1051 (2008).
39. S. Terryn, G. Mathijssen, J. Brancart, T. Verstraten, G. Van Assche, B. Vanderborght, Toward self-healing actuators: A preliminary concept. *IEEE Trans. Robot.* **32**, 736–743 (2016).
40. S. Terryn, G. Mathijssen, J. Brancart, G. Van Assche, B. Vanderborght, D. Lefeber, Investigation of self-healing compliant actuators for Robotics, in *Proceedings of IEEE International Conference on Robotics Automation (ICRA)* (IEEE, 2015), pp. 258–263.
41. F. Ilievski, A. D. Mazzeo, R. F. Shepherd, X. Chen, G. M. Whitesides, Soft robotics for chemists. *Angew. Chem.* **123**, 1930–1935 (2011).
42. Y. Sun, Y. Seong Song, J. Paik, Characterization of silicone rubber based soft pneumatic actuators, in *Proceedings of International Conference on Intelligent Robots and Systems (IROS)* (IEEE, 2013), pp. 4446–4453.
43. G. K. Klute, B. Hannaford, Accounting for elastic energy storage in McKibben artificial muscle actuators. *J. Dyn. Syst. Meas. Control* **122**, 386–388 (2000).
44. B. Verrelst, R. Van Ham, Second generation pleated pneumatic artificial muscle and its robotic applications. *Adv. Robot.* **20**, 783–805 (2006).
45. F. Daerden, D. Lefeber, The concept and design of pleated pneumatic artificial muscles. *Int. J. Fluid Power* **2**, 41–50 (2001).

Funding: This research is funded by the European Commission ERC Starting Grant "Series-Parallel Elastic Actuation for Robotics" (SPEAR) (no. 337596). S.T. is funded by the PhD Fellowship of the Research Foundation Flanders (FWO). **Author contributions:** S.T. designed and performed all experiments. J.B. assisted in characterizing the DA polymers. All authors contributed in the writing of the paper. **Competing interests:** The authors declare that they have no competing interests. **Data and materials availability:** All data supporting conclusions can be found in the Supplementary Materials. For more detailed information on materials and methods, contact S.T. (seterryn@vub.ac.be).

Submitted 14 April 2017
Accepted 20 July 2017
Published 16 August 2017
10.1126/scirobotics.aan4268

Citation: S. Terryn, J. Brancart, D. Lefeber, G. Van Assche, B. Vanderborght, Self-healing soft pneumatic robots. *Sci. Robot.* **2**, eaan4268 (2017).

Downloaded from https://www.science.org at The Hong Kong University of Science and Technology (Guangzhou) on May 26, 2026

Science Robotics

Self-healing soft pneumatic robots

Seppe Terryn, Joost Brancart, Dirk Lefeber, Guy Van Assche, and Bram Vanderborght

Sci. Robot. **2** (9), eaan4268. DOI: 10.1126/scirobotics.aan4268

View the article online
https://www.science.org/doi/10.1126/scirobotics.aan4268
Permissions
https://www.science.org/help/reprints-and-permissions

Downloaded from https://www.science.org at The Hong Kong University of Science and Technology (Guangzhou) on May 26, 2026

Use of this article is subject to the Terms of service

Science Robotics (ISSN 2470-9476) is published by the American Association for the Advancement of Science. 1200 New York Avenue NW, Washington, DC 20005. The title *Science Robotics* is a registered trademark of AAAS.

Copyright © 2017 The Authors, some rights reserved; exclusive licensee American Association for the Advancement of Science. No claim to original U.S. Government Works